

# 000 001 002 003 004 005 006 007 008 009 010 NAVIGATING THE ACCURACY-SIZE TRADE-OFF WITH FLEXIBLE MODEL MERGING

005 **Anonymous authors**

006 Paper under double-blind review

## ABSTRACT

011 Model merging has emerged as an efficient method to combine multiple single-task  
 012 fine-tuned models. The merged model can enjoy multi-task capabilities without  
 013 expensive training. While promising, merging into a single model often suffers from  
 014 an accuracy gap with respect to individual fine-tuned models. On the other hand,  
 015 deploying all individual fine-tuned models incurs high storage costs. We propose  
 016 **FLEXMERGE**, a novel data-free model merging framework that: *(a)* flexibly generates  
 017 merged models of varying sizes, spanning the full spectrum from a single merged  
 018 model to retaining all individual fine-tuned models; and *(b)* supports multiple  
 019 merging algorithms in a unified framework. Using **FLEXMERGE**, we systematically  
 020 characterize the accuracy–size trade-off of different algorithms. Our study reveals  
 021 two key findings: first, even modestly larger merged models can yield steep  
 022 accuracy gains (up to 13.5% when just doubling the size); second, algorithm  
 023 rankings are not consistent as size increases, with some methods overtaking others  
 024 beyond the one-model regime. These results uncover a new design dimension for  
 025 model merging: developing and comparing algorithms across the full spectrum of  
 026 sizes rather than only at the single-model limit. Extensive experiments on vision  
 027 and NLP benchmarks, with up to 30 tasks, confirm the generality and practicality  
 028 of **FLEXMERGE**.

## 029 1 INTRODUCTION

030 In recent years, the pre-training followed by fine-tuning paradigm has become the leading approach  
 031 in both natural language processing (NLP) and computer vision, showcasing remarkable success on a  
 032 wide range of tasks (Devlin et al., 2018; Dodge et al., 2020; Dosovitskiy et al., 2021; Bommasani et al.,  
 033 2021). Pre-trained models (PTMs), which learn generalized features from large-scale datasets, serve  
 034 as powerful starting points, enabling fine-tuning to achieve superior performance on downstream  
 035 tasks with less labeled data. This has led to an exponential growth in the number of fine-tuned models  
 036 driven further by the availability of open-source repositories (maintainers & contributors, 2016; Wolf  
 037 et al., 2019). However, *deploying individual fine-tuned models* for specific tasks incurs high storage  
 038 and deployment costs. The alternative is Multi-task learning (MTL), which aims to jointly train *a*  
 039 *single model* across multiple tasks (Vandenhende et al., 2021; Sanh et al., 2022). But MTL comes  
 040 with its own drawbacks, such as significant computational overhead and the need to simultaneously  
 041 access the data from all tasks, which might be infeasible due to privacy constraints (Jin et al., 2023).

042 To mitigate these limitations, model merging has emerged as a promising solution, allowing the  
 043 combination of multiple fine-tuned models into a *single model* without access to training data. To this  
 044 end, several model merging methods have been proposed (Gargiulo et al., 2025; Huang et al., 2024;  
 045 Yang et al., 2024a; Yadav et al., 2023; Ilharco et al., 2023; Matena & Raffel, 2022). However, a single  
 046 model is often unable to perfectly resolve parameter conflicts between tasks, leaving an accuracy gap  
 047 with respect to the individual fine-tuned models (Zhang et al., 2025; Huang et al., 2024). This gap  
 048 becomes more significant as a higher number of models are merged (Yadav et al., 2023; Ilharco et al.,  
 049 2023). To mitigate this issue, some methods leverage additional data to facilitate merging (Lu et al.,  
 050 2024; Yang et al., 2024a; Tang et al., 2024a; Yang et al., 2024b). Yet, the data-dependency might be  
 051 difficult to meet in practice due to privacy constraints or proprietary restrictions, leading to a growing  
 052 focus on data-free model merging techniques (Gargiulo et al., 2025; Huang et al., 2024; Du et al.,  
 053 2024; Yu et al., 2024; Yadav et al., 2023). Nevertheless, in the absence of data, the accuracy gap  
 remains significant, highlighting the need for novel solutions.

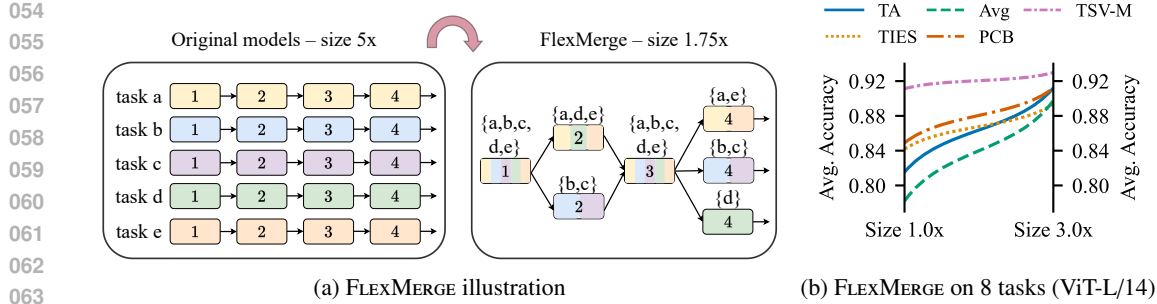


Figure 1: (a) Fine-tuned models are sequences of blocks. FLEXMERGE iteratively merges block pairs until reaching the desired size (e.g., size  $1.75\times$ ). (b) Algorithm rankings change as size is increased.

We argue that an effective solution to this challenge is to go beyond the conventional one model approach, and merge into model(s) of bigger sizes. Merging multiple fine-tuned models naturally presents a trade-off between maintaining accuracy and achieving model compactness, dictated by the size of the merged model. This trade-off spans a spectrum: at one extreme, retaining all individual fine-tuned models for each task achieves maximal accuracy but at the cost of larger overall size; at the other, fully merging all tasks into a single model minimizes storage size but sacrifices accuracy. Despite this clear trade-off, a systematic investigation of the accuracy-size relationship in model merging has been lacking. In this light, we pose two key research questions: *(RQ1) How can we derive merged models across the full range of model sizes in a data-free manner?* and *(RQ2) What is the nature of the accuracy-size trade-off exhibited by different data-free merging algorithms?*

In response to (RQ1), we propose FLEXMERGE, a flexible framework that enables *data-free* fusion into model(s) of any desired size. At its core, FLEXMERGE treats each fine-tuned model as composed of sequential blocks, as illustrated in Figure 1(a), whose granularity can be controlled (e.g., a transformer block, a few layers, or even a single layer). It then takes a bottom-up approach starting with all fine-tuned models with their respective blocks and greedily merging a pair of blocks with the highest cosine similarity in each merging iteration. This merging can leverage *any* existing data-free merging method such as Task Arithmetic (TA) (Ilharco et al., 2023), TIES-MERGING (Yadav et al., 2023), EMR-MERGING (Huang et al., 2024), TSV-M (Gargiulo et al., 2025), etc., applied at the block-level. With each merging iteration, the size of the deployed model is reduced, and the process can be halted once the desired size is met. For instance, in Figure 1(a), the merging is halted when the merged model is  $1.75\times$  the size of a single fine-tuned model. The entire merging process in FLEXMERGE needs no additional data or tuning, making FLEXMERGE fully *data-free*.

In response to (RQ2), we demonstrate with FLEXMERGE that a range of data-free merging algorithms exhibit highly favorable accuracy-size trade-offs. Remarkably, the accuracy-size trade-off is characterized by steep gains in accuracy for even modestly bigger merged models beyond one model, followed by steady improvements, reaching near fine-tuning accuracy well before the maximum size. To illustrate this in practice, Figure 2 charts the merged model accuracy versus deployed size for 8 tasks (top) and 30 tasks (bottom) using the ViT-B/32 model, with TA (Ilharco et al., 2023) and CONSENSUS (Wang et al., 2024) as the respective merging methods.  $\circ$  and  $\square$  annotate the accuracy at both ends of the spectrum *i.e.*, lowest fused size and retaining all fine-tuned models respectively. FLEXMERGE + TA gains 13.5% in average accuracy when going from  $1\times$  to  $2\times$  while FLEXMERGE + CONSENSUS gains 8.5% when doubling the size from approximately  $3\times$  to  $6\times$ . We note that CONSENSUS requires storing masks and the pre-trained parameters alongside the unified parameters (Wang et al., 2024), resulting in the lowest possible size of  $\approx 3\times$  for 30 tasks. We observe that the steep rise is followed by relatively slower accuracy

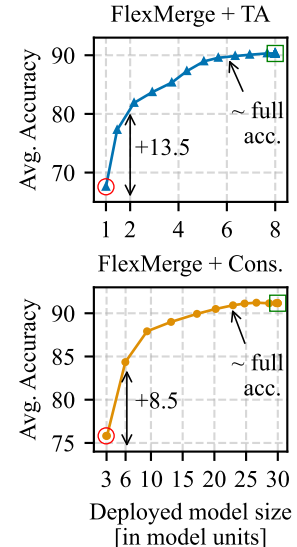


Figure 2: FLEXMERGE enables large accuracy gains when just doubling the deployed model size and attains full accuracy well before the maximum size.

108 growth in the middle. Yet, a near fine-tuning accuracy is attained well before the maximum size. For  
 109 8 tasks, this is obtained around size  $6\times$  and for 30 tasks, around size  $23.5\times$ . Secondly, we observe  
 110 that algorithm rankings are not consistent even at modestly bigger sizes. Figure 1(b) shows that  
 111 vanilla averaging exceeds TIES-MERGING while TA attains the performance of PCB-MERGING at size  
 112  $3\times$  despite starting from a large gap at  $1\times$ . *Our findings open a new design dimension: encouraging*  
 113 *algorithm development and comparison for sizes  $> 1\times$  instead of restricting only to  $1\times$ .*

114 **Contributions.** To the best of our knowledge, we present the first study of model merging that:

115

- 116 • Generates merged models across full spectrum of sizes, *including non-integer sizes*;
- 117 • Supports a wide range of data-free merging algorithms, *within a unified framework*;
- 118 • Provides a systematic characterization of the accuracy-size trade-off in data-free model merging,  
   *revealing general trends, highly favorable regions and inconsistency of algorithm rankings*;
- 119 • Demonstrates that larger merged sizes incur negligible inference-time overhead, *enabled by our*  
   *efficient implementation*.

120  
 121 We confirm our findings through extensive experiments spanning language and vision modalities,  
 122 multiple model families, multi-modal datasets, using both full-parameter fine-tuning (FFT) and  
 123 parameter efficient fine-tuning (PEFT), scaling up to 30 tasks.

## 124 2 RELATED WORK

125 Initial studies on model merging focused on vanilla averaging as a way of combining models obtained  
 126 from same or different training runs of a task into one higher performing model (Izmailov et al.,  
 127 2018; Gupta et al., 2020; Wortsman et al., 2022; Cha et al., 2021). Vanilla averaging is also used in  
 128 federated learning to merge different client models (McMahan et al., 2017; Konečný et al., 2016).  
 129 Ilharco et al. (2023) introduced task vectors, representing the difference between fine-tuned and  
 130 pre-trained models, enabling model combination through vector arithmetic.

131 **Data-based merging** methods leverage validation data to facilitate merging. Techniques like **FISHER**  
 132 **MERGING** (Matena & Raffel, 2022) and **REGMEAN** (Jin et al., 2023) compute the Fisher Information  
 133 and Gram matrices, respectively, for weighted averaging of model parameters. **SURGERY** (Yang et al.,  
 134 2024a) trains task-specific adapters to debias the representations produced by the merged model.  
 135 **ADAMERGING** (Yang et al., 2024b) introduces per-task, per-layer merging co-efficients, and proposes  
 136 to learn these co-efficients by solving an entropy minimization objective. **WEMoE** (Tang et al.,  
 137 2024a) merges all modules except for task-specific MLPs, which are retained as weight-ensembled  
 138 mixture-of-experts (MoE) with learned routers. **TWIN-MERGING** (Lu et al., 2024) leverages MoE on  
 139 difference vectors *i.e.*, the difference between the fine-tuned models and the merged model. While the  
 140 availability of validation data enhances accuracy, such data might be difficult to obtain in practice.

141 **Data-free merging** directly merges model parameters without any data. **TIES-MERGING** (Yadav  
 142 et al., 2023) resolves parameter interference by trimming redundant parameters and resolving sign  
 143 conflicts. **PCB-MERGING** (Du et al., 2024) considers both intra- and inter-parameter competition  
 144 balancing. **DARE** (Yu et al., 2024) reduces parameter interference by randomly dropping parameters  
 145 and proportionally rescaling remaining ones. **EMR-MERGING** (Huang et al., 2024) introduces the  
 146 paradigm of maintaining light-weight task specific masks in addition to the merged model to enhance  
 147 performance. **CONSENSUS** (Wang et al., 2024) also relies on task specific masks, but creates them  
 148 differently compared to **EMR-MERGING**. Both approaches significantly improve accuracy over  
 149 previous methods, albeit at the cost of test-time reconstruction overhead (Gargiulo et al., 2025).  
 150 **TSV-M** (Gargiulo et al., 2025) merges SVD-decomposed task singular vectors, reducing interference  
 151 by retaining only prominent singular directions and orthogonalizing them across tasks.

152 Recent work by Zhang et al. (2025) explores merging into sizes  $> 1\times$ . Their method, **CHANNEL**  
 153 **MERGING**, relies on layer-wise K-Means clustering followed by merging within each cluster using  
 154 only TA. However, this approach is restrictive as it cannot generate fractional-sized models. Despite  
 155 the emergence of advanced methods and attempts at merging into bigger sizes, to the best of our  
 156 knowledge, no prior work has systematically investigated the accuracy-size trade-off in model  
 157 merging under a single unified framework. For completeness, we provide additional related work and  
 158 a taxonomy of existing algorithms based on their data-free/data-based nature in Appendix A.

162 

### 3 FLEXMERGE

164 

#### 3.1 PRELIMINARIES

166 We consider a set of  $M$  tasks:  $\{T_1, \dots, T_M\}$ , where the fine-tuned model parameters for task  $T_i$  are  
 167 denoted by  $\theta_i$ . These fine-tuned parameters are typically obtained by adapting a pre-trained model,  
 168 such as ViT (Dosovitskiy et al., 2021) or T5 (Raffel et al., 2020) using either full parameter fine-  
 169 tuning (FT) or parameter-efficient fine-tuning (PEFT) methods (Liu et al., 2022). Thus, it is assumed  
 170 that all the fine-tuned models have the same size and the model architecture as the pre-trained model,  
 171 as also considered in prior work (Ilharco et al., 2023; Yadav et al., 2023). To analyze the changes  
 172 introduced by fine-tuning, we use the concept of task vectors  $\tau_i$  introduced by Ilharco et al. (2023),  
 173 where  $\tau_i = \theta_i - \theta_{\text{pre}}$ , with  $\theta_{\text{pre}}$  being the pre-trained weights. These task vectors capture the specific  
 174 modifications needed for each task and provide a compact representation for merging.

175 Standard model merging approaches involve combining the task-vectors  $\{\tau_1, \dots, \tau_M\}$  into a unified  
 176 task vector  $\tau_{\text{uni}} = \mathcal{F}(\{\tau_1, \dots, \tau_M\})$  and then adding the unified task vector to the pre-trained weights  
 177 to get the final merged model,  $\theta_{\text{uni}} = \theta_{\text{pre}} + \tau_{\text{uni}}$ . Here  $\mathcal{F}$  denotes the merging algorithm used to  
 178 obtain the unified task vector's weights. For example, the unified task vector  $\tau_{\text{uni}}$  can be computed via  
 179 simple averaging  $\tau_{\text{uni}} = \frac{1}{M} \sum_{i=1}^M \tau_i$  or via TA (Ilharco et al., 2023) that uses a coefficient  $\lambda$  to weigh  
 180 the contribution<sup>1</sup> of the unified task vector  $\tau_{\text{uni}} = \lambda \cdot \frac{1}{M} \sum_{i=1}^M \tau_i$  in the final merged model. It is shown  
 181 that just by tuning  $\lambda$ , one can outperform weight averaging (Ilharco et al., 2023).

182 **Motivation.** Merging into one model  $\theta_{\text{uni}}$  may cause accuracy deterioration due to parameter  
 183 interference between different fine-tuned models (Zhang et al., 2025; Yadav et al., 2023). This  
 184 behavior becomes prominent as more and more fine-tuned models are merged, as discussed in  
 185 Section 1. On the other hand, retaining all fine-tuned models preserves full fine-tuning accuracy  
 186 but results in a net size  $M \times$  that of one fine-tuned model, which is impractical due to the high  
 187 memory requirements. In this work, we investigate the problem of generating models of any  
 188 desired size in the range  $[1, M]$ , including models with fractional size such as  $2.25 \times$  model units.

190 

#### 3.2 PROPOSED APPROACH

192 To enable a more granular fusion,  
 193 we consider the model to be com-  
 194 posed of  $B$  sequential blocks, for  
 195 instance transformer blocks in a  
 196 ViT model or even layers within  
 197 each transformer block such as at-  
 198 tention or MLP layers could be  
 199 considered as unique blocks. As-  
 200 suming  $B$  total blocks, we consider  
 201 the task vectors for each block as  

$$\{\tau_k^b\}_{b=1}^B$$
 corresponding to the origi-  
 202 nal task vector  $\tau_k$  for a task  $k$ . Our  
 203 proposed framework, FLEXMERGE,  
 204 takes a greedy approach to effi-  
 205 ciently merge task vectors from  
 206 multiple tasks at the granularity of  
 207 blocks, aiming to reduce the de-  
 208 ployed model size while main-  
 209 taining utility. The pseudo-code for  
 210 FLEXMERGE is presented in Algo-  
 211 rithm 1.

---

**Algorithm 1: FLEXMERGE framework**

---

**Input:** Task vectors  $\{\tau_k^b\}$  for all  $k \in [M], b \in [B]$ ;  
 merging algorithm  $\mathcal{F}$ ; target size  $S_{\text{target}}$   
**Output:** Merged task vectors with reduced size

---

1  $S \leftarrow 0$  ▷ Initialize deployed size  
 2 **for**  $b = 1$  **to**  $B$  **do**  
 3    $\mathcal{G}^b \leftarrow \emptyset$   
 4   **for**  $k = 1$  **to**  $M$  **do**  
 5      $\mathcal{G}^b \leftarrow \mathcal{G}^b \cup (\{k\}, \tau_k^b)$   
 6      $S \leftarrow S + \text{size}(\tau_k^b)$   
 7 **while**  $S > S_{\text{target}}$  **or not all blocks merged do**  
 8   Find block  $b^*$  and pair  $(g_{i^*}, g_{j^*}) \in \mathcal{G}^{b^*}$  with the  
   highest similarity:  
 9   
$$(b^*, g_{i^*}, g_{j^*}) = \arg \max_{b \in [B], g_i, g_j \in \mathcal{G}^b} \text{SIMILARITY}(g_i, g_j)$$
  
 10    $\mathcal{T}_{i^*}^{b^*}, \mathcal{T}_{j^*}^{b^*} \leftarrow g_{i^*}(0), g_{j^*}(0)$  ▷ Get task subsets  
 11    $\mathcal{T}_{\text{uni}}^{b^*} \leftarrow \mathcal{T}_{i^*}^{b^*} \cup \mathcal{T}_{j^*}^{b^*}$  ▷ Merge task subsets  
 12    $\tau_{\text{uni}}^{b^*} \leftarrow \mathcal{F}(\{\tau_k^{b^*} \mid k \in \mathcal{T}_{\text{uni}}^{b^*}\})$  ▷ Merge task vectors  
 13    $\mathcal{G}^{b^*} \leftarrow \mathcal{G}^{b^*} \cup (\mathcal{T}_{\text{uni}}^{b^*}, \tau_{\text{uni}}^{b^*}) \setminus \{g_{i^*}, g_{j^*}\}$  ▷ Update the block  
 14    $S \leftarrow S - \text{size}(\tau_{\text{uni}}^{b^*})$  ▷ Update current size

---

215 <sup>1</sup>We add a scaling factor of  $1/M$  to the standard definition  $\tau_{\text{uni}} = \lambda \cdot \sum_{i=1}^M \tau_i$  given in (Ilharco et al., 2023) to  
 better suit its usage in FLEXMERGE where  $M$  can vary across blocks.

216 **Initialization (Lines 1–6).** The merging proceeds bottom-up. Initially, no merging has occurred,  
 217 and we retain  $\tau_k^b$  for all tasks  $k \in [M]$  and all blocks  $b \in [B]$  (see Figure 1(a)). For each block  
 218  $b$ , we initialize a set of tuples:  $\mathcal{G}^b = \{(\{k\}, \tau_k^b) \mid k \in [M]\}$ . Each tuple in  $\mathcal{G}^b$  consists of: (i) a task  
 219 set  $\{k\}$  (tracking which tasks are represented) and (ii) the corresponding block task vector  $\tau_k^b$ . For  
 220 example, in Figure 1(a) for the first block, we would have  $\mathcal{G}^1 = \{(\{a\}, \tau_a^1), \dots, (\{e\}, \tau_e^1)\}$ . When the  
 221 merging terminates, the resulting  $\mathcal{G}^1$  for Figure 1(a) would be  $\mathcal{G}^1 = \{(\{a, \dots, e\}, \hat{\tau}_{\text{uni}}^1)\}$ , where  $\hat{\tau}_{\text{uni}}^1$  is  
 222 the merged task vector for the first block for all tasks. The initial size  $S$  is calculated as the cumulative  
 223 size of all block parameters across  $M$  tasks.  
 224

225 **Iteration (lines 7–14).** In each iteration, the algorithm identifies a block  $b^*$  and pair of tuples  
 226  $(g_{i^*}, g_{j^*}) \in \mathcal{G}^{b^*}$ , which have the highest similarity (as defined below). Then they are merged as  
 227 follows. Let  $\mathcal{T}_{i^*}^{b^*}$  and  $\mathcal{T}_{j^*}^{b^*}$  be the subset of tasks associated with  $g_{i^*}$  and  $g_{j^*}$  respectively, *i.e.*, the  
 228 first elements of  $g_{i^*}$  and  $g_{j^*}$  respectively. First,  $\mathcal{T}_{i^*}^{b^*}$  and  $\mathcal{T}_{j^*}^{b^*}$  are merged via a union operation:  
 229  $\mathcal{T}_{\text{uni}}^{b^*} = \mathcal{T}_{i^*}^{b^*} \cup \mathcal{T}_{j^*}^{b^*}$ . Next, the merged task vector corresponding to block  $b^*$  and set  $\mathcal{T}_{\text{uni}}^{b^*}$  is created as  
 230 follows:  $\tau_{\text{uni}}^{b^*} = \mathcal{F}(\{\tau_k^{b^*} \mid k \in \mathcal{T}_{\text{uni}}^{b^*}\})$ . Here  $\mathcal{F}$  can be *any* data-free merging algorithm. The tuple set  
 231  $\mathcal{G}^{b^*}$  is then updated by removing the tuples  $g_{i^*}, g_{j^*}$  and adding the new merged tuple  $(\mathcal{T}_{\text{uni}}^{b^*}, \tau_{\text{uni}}^{b^*})$ . Each  
 232 merge reduces the model size by the size of the task vector corresponding to block  $b^*$ , and the process  
 233 continues until the current size  $S$  meets the desired size  $S_{\text{target}}$  or no further merges are possible.  
 234

235 **Similarity function.** We measure the similarity between two groups  $g_i, g_j$  in any block  $b$  using the  
 236 lowest cosine similarity between any pair of original task vectors corresponding to the tasks in the  
 237 sets  $\mathcal{T}_i^b$  and  $\mathcal{T}_j^b$ :

$$\text{SIMILARITY}(g_i, g_j) = \min_{k_1 \in \mathcal{T}_i^b, k_2 \in \mathcal{T}_j^b} \text{cosine\_sim}(\tau_{k_1}^b, \tau_{k_2}^b). \quad (1)$$

238 Our choice of the min similarity derives from our ablations comparing different strategies—max, min,  
 239 and average—as well as computing similarity between merged group task vectors directly. Among  
 240 these, min yields the best performance. Thus at each iteration, we merge the pair of groups with the  
 241 highest of these minimum similarities (line 9, Algorithm 1). While the cosine similarity between full  
 242 task vectors can be relatively low (Ilharco et al., 2023), the block-level similarities tend to be higher  
 243 and effective for merging. CHANNEL MERGING (Zhang et al., 2025) also employs cosine similarity.  
 244

245 **Enhancing efficiency.** The pairwise similarities can be precomputed once for all pairs and accessed  
 246 in constant time during the merging process. Furthermore, we leverage the Disjoint Set Union  
 247 (DSU) (Cormen et al., 2009) data structure to efficiently track and unify task sets for each block. Our  
 248 design enables FLEXMERGE to perform very efficient merging even under many tasks (see Table 2).  
 249

250 **Complexity Analysis.** Algorithm 1 identifies most similar block pairs in each iteration. We presented  
 251 the algorithm in this form for conceptual clarity. However, in practice, we generate the global merging  
 252 order for all blocks first and then apply merges. To analyze the time complexity of FLEXMERGE, we  
 253 consider three distinct stages of this process: similarity pre-computation, generating merging order,  
 254 and actual parameter merging.  
 255

- 256 • **Similarity pre-computation:** We compute the pairwise cosine similarities between  $M$  tasks in  
 257 each block, across all  $B$  blocks. Let the maximum size of any block task vector be  $d_{\text{max}}$ , then the  
 258 similarity computes takes  $O(d_{\text{max}})$  per pair. With  $\binom{M}{2}$  pairs per block, this step is  $O(BM^2 d_{\text{max}})$ .  
 259
- 260 • **Generating merging order:** Our greedy merging using Equation (1) is an instance of a specific  
 261 form of clustering, called single-linkage clustering. We thus use the SLINK algorithm (Sibson,  
 262 1973) which takes as input the similarity matrix and generates a sorted list of merge orders for  
 263 each block in  $O(M^2)$ . For  $B$  blocks, this takes  $O(BM^2)$ . We then need to combine these per-block  
 264 sorted lists, each of size  $M - 1$ , into a single global sorted list. Using a min-heap, this takes  
 265  $O(BM \log B)$  (Knuth, 1997). In total, this step takes  $O(BM^2 + BM \log B)$  and results in a global  
 266 merge ordering across all blocks.  
 267
- 268 • **Applying parameter merging:** We now merge the blocks in the generated order. For linear  
 269 algorithms like TA, merging a group  $g$  of size  $|g|$  with task vectors of size  $d$  takes  $O(|g|d)$ . Summing  
 270 over all groups  $\mathcal{G}^b$  within a block takes  $\sum_{g \in \mathcal{G}^b} O(|g| \cdot d) = O((\sum_{g \in \mathcal{G}^b} |g|)d) = O(Md)$ . Repeating this  
 271 for  $B$  blocks and upper bounding  $d$  with  $d_{\text{max}}$  results in  $O(BMd_{\text{max}})$ .  
 272

270 Table 1: Summary of existing data-free merging methods. Column  $\mathcal{F}(\{\tau_k^b \mid k \in \mathcal{T}_{\text{uni}}^b\})$  denotes the  
 271 result of merging. Figure 7 (Section B) provides an illustrative diagram.  
 272

273	Algorithm	$\mathcal{F}(\{\tau_k^b \mid k \in \mathcal{T}_{\text{uni}}^b\})$	Final Model	What is stored?
274	TA (Ilharco et al., 2023), TIES (Yadav et al., 2023), Avg. (Ilharco et al., 2023), PCB (Du et al., 2024), TSV-M (Gargiulo et al., 2025)	$\tau_{\text{uni}}^b$	$\theta_{\text{uni}}^b = \theta_{\text{pre}}^b + \tau_{\text{uni}}^b$	$\theta_{\text{uni}}^b$
277	CONSENSUS (Wang et al., 2024)	$\tau_{\text{uni}}^b, \{m_k^b \mid k \in \mathcal{T}_{\text{uni}}^b\}$	$\hat{\theta}_k^b = \theta_{\text{pre}}^b + \tau_{\text{uni}}^b \circ m_k^b$ (reconstructed per-task $k$ )	$\theta_{\text{pre}}^b, \tau_{\text{uni}}^b, \{m_k^b \mid k \in \mathcal{T}_{\text{uni}}^b\}$
279	EMR-MERGING (Huang et al., 2024)	$\tau_{\text{uni}}^b, \{m_k^b, \gamma_k^b \mid k \in \mathcal{T}_{\text{uni}}^b\}$	$\hat{\theta}_k^b = \theta_{\text{pre}}^b + \gamma_k^b \cdot \tau_{\text{uni}}^b \circ m_k^b$ (reconstructed per-task $k$ )	$\theta_{\text{pre}}^b, \tau_{\text{uni}}^b, \{m_k^b, \gamma_k^b \mid k \in \mathcal{T}_{\text{uni}}^b\}$

282 The total complexity is dominated by the similarity pre-computation (as  $d_{\text{max}}$  is typically larger than  
 283  $B$ ), resulting in a final complexity of  $O(BM^2d_{\text{max}})$ . Note however that  $d_{\text{max}}$  is much smaller than the  
 284 total model dimension, at it only corresponds to the maximum size of any block of the model.

### 286 3.3 EXISTING MERGING METHODS IN COMBINATION WITH FLEXMERGE

288 FLEXMERGE provides the flexibility to choose any data-free merging algorithm  $\mathcal{F}$  from a diverse  
 289 set of existing approaches. Unlike traditional methods that operate at the level of full task vectors,  
 290 FLEXMERGE applies merging algorithms at the block level, fusing block task vectors. We detail the  
 291 exact block-level merging procedure for different algorithms next. In standard approaches like TA,  
 292 TSV-M, and PCB-MERGING, task vectors are merged into a single unified task vector. When applied  
 293 at the block-level, the merging outcome for any block  $b$  can be denoted as:  $\tau_{\text{uni}}^b \leftarrow \mathcal{F}(\{\tau_k^b \mid k \in \mathcal{T}_{\text{uni}}^b\})$   
 294 where  $\mathcal{F}$  is the specific merging algorithm and  $\mathcal{T}_{\text{uni}}^b$  is the subset of tasks for which the merging  
 295 occurs. The final block parameters are then computed as  $\theta_{\text{uni}}^b = \theta_{\text{pre}}^b + \tau_{\text{uni}}^b$ . Approaches such as  
 296 CONSENSUS generate task-specific masks in addition to the unified vector:  $\tau_{\text{uni}}^b, \{m_k^b \mid k \in \mathcal{T}_{\text{uni}}^b\} \leftarrow$   
 297  $\mathcal{F}(\{\tau_k^b \mid k \in \mathcal{T}_{\text{uni}}^b\})$ . Then during inference, the task-specific weights for task  $k$  are reconstructed as  
 298  $\hat{\theta}_k^b = \theta_{\text{pre}}^b + \tau_{\text{uni}}^b \circ m_k^b$ . CONSENSUS thus stores  $\theta_{\text{pre}}^b, \tau_{\text{uni}}^b$ , and the binary masks  $\{m_k^b \mid k \in \mathcal{T}_{\text{uni}}^b\}$  and  
 299 defers per-task reconstruction to the inference time. This leads to a storage cost exceeding 2 $\times$  that  
 300 of standard methods, which only store  $\theta_{\text{uni}}^b$ . EMR-MERGING further generates task-specific scalars  
 301  $\{\gamma_k^b \mid k \in \mathcal{T}_{\text{uni}}^b\}$  in addition to the masks, however the storage cost of these scalars is negligible. Table 1  
 302 summarizes the merging outcomes for different algorithms, applied at block-level within FLEXMERGE.  
 303 Figure 7 (Section B) provides an illustrative diagram.

## 305 4 EXPERIMENTS

307 We split our evaluation as follows: (i) Merging on vision, PEFT and FFT benchmarks in Section 4.1;  
 308 (ii) FLEXMERGE vs CHANNEL MERGING in Section 4.2; and (iii) ablation and efficiency analysis in  
 309 Section 4.3. Lastly, multi-modal and OOD results are in Appendices C.4 and C.6.<sup>2</sup>

310 **Merging algorithms.** We investigate the accuracy-size trade-off for several data-free merging  
 311 algorithms including Vanilla Averaging, TA (Ilharco et al., 2023), TIES-MERGING (Yadav et al., 2023),  
 312 PCB-MERGING (Du et al., 2024), TSV-M (Gargiulo et al., 2025), CONSENSUS (Wang et al., 2024) and  
 313 EMR-MERGING (Huang et al., 2024) on extensive vision and NLP benchmarks. As noted earlier,  
 314 the focus of our work is data-free model merging. Hence, existing data-based algorithms such as  
 315 SURGERY (Yang et al., 2024a), ADAMERGING (Yang et al., 2024b), TWIN-MERGING (Lu et al., 2024), etc.  
 316 are not directly comparable in our setting.

317 **Hyperparameters.** For TA, we set  $\lambda = 1.5$ . For TIES-MERGING, we use a sparsity ratio of 0.1 and  
 318 employ the recommended value of  $\lambda = 1$ . For CONSENSUS, we set the hyperparameter responsible for  
 319 controlling the amount of information extracted by masks to 0.6 for all tasks and use TIES-MERGING  
 320 as the algorithm to generate unified task vectors. For FLEXMERGE, we set the block granularity at  
 321 the level of individual components within the transformer layer, *i.e.*, the attention, MLP, and layer  
 322 normalization modules are treated as separate blocks during the merging process.

323 <sup>2</sup>Our anonymized code is available at: <https://anonymous.4open.science/r/model-merging-84F2>

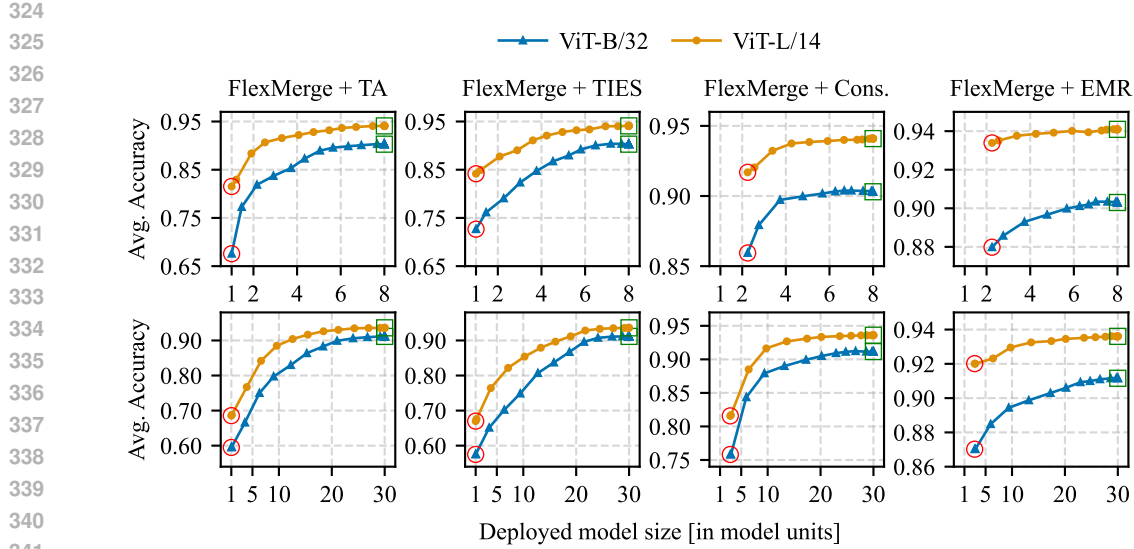


Figure 3: Merging 8 (top) and 30 (bottom) tasks. The accuracy-size trade-off shows rapid initial gains, followed by gradual improvement, reaching near fine-tuning accuracy well before the maximum size.

#### 4.1 MERGING RESULTS

**Merging 8 and 30 vision models.** For the image classification tasks, we follow the setup from existing work (Huang et al., 2024; Yadav et al., 2023). Specifically, we use two versions of the CLIP model (Radford et al., 2021), incorporating ViT-B/32 and ViT-L/14 as visual encoders (Dosovitskiy et al., 2021). We evaluate on the standard 8 task benchmark (Ilharco et al., 2023) as well as an extended 30 task benchmark (detailed in Appendix B.2). Figure 3 plots average accuracy vs. deployed model size (in multiples of a single fine-tuned model). For FLEXMERGE + TA, the accuracy increases fairly rapidly as the model size grows beyond 1 $\times$ . The gains are significant (top row), where the accuracy reaches  $> 80\%$  at size 2 $\times$  from only 67.5% at size 1 $\times$  for the ViT-B/32 model in the 8 task setup. Similar gains are also observed for 30 tasks (bottom row).

Masking-based approaches, CONSENSUS and EMR-MERGING, begin with substantially higher accuracy than TA and TIES-MERGING, but their smallest size exceeds 1 $\times$  due to the need to store pre-trained weights and binary masks (Section 3.3). On 8 tasks, CONSENSUS was shown to match fine-tuned accuracy at small sizes, but only when its extraction parameter is separately tuned per task (Wang et al., 2024). FLEXMERGE + CONSENSUS also shows strong gains, improving from 76% at  $\approx 3\times$  to 84.5% at  $\approx 6\times$  for ViT-B/32 in 30 tasks. EMR-MERGING maintains high accuracy even at the smallest size. Yet, it exhibits an accuracy gap w.r.t. the fine-tuned models, which can be effectively reduced by increasing the deployed model size. Larger ViT-L/14 models achieve higher accuracy across all methods, but the accuracy-size trade-off remains similar: rapid initial gains followed by gradual improvements. Most algorithms approach the fine-tuning accuracy (denoted by  $\square$ ) well before maximum size, around 6 $\times$  for 8 tasks and 23.5 $\times$  for 30 tasks. Thus, in cases requiring storage of all fine-tuned models, FLEXMERGE can reduce size by about 25% with little accuracy loss.

**Merging 11 PEFT models.** We adopt the experimental setup from prior work (Huang et al., 2024; Yadav et al., 2023). Specifically, we employ the (IA)<sup>3</sup> (Liu et al., 2022) PEFT method on the T0-3B (Sanh et al., 2022) base model using 11 diverse datasets sourced from (Yadav et al., 2023) (detailed in Section B.3). Figure 4(a) demonstrates the benefits of deploying larger model sizes, where in this case the model size is measured with respect to the (IA)<sup>3</sup> modules. FLEXMERGE + TA achieves notable gains, increasing accuracy from 59% at size 1 $\times$  to 66.2% at 3 $\times$ , a 7.2% improvement. Similarly, FLEXMERGE + EMR-MERGING surpasses 70% accuracy at 5 $\times$ , starting from 67.6% at the lowest size of 2.34 $\times$ . We observe similar trends for other algorithms, included in Appendix C.2.

**Merging 7 FFT models.** For this experiment, we closely follow the setup from prior work (Du et al., 2024; Yadav et al., 2023). We use T5-Base and T5-Large as base models, applying full-parameter

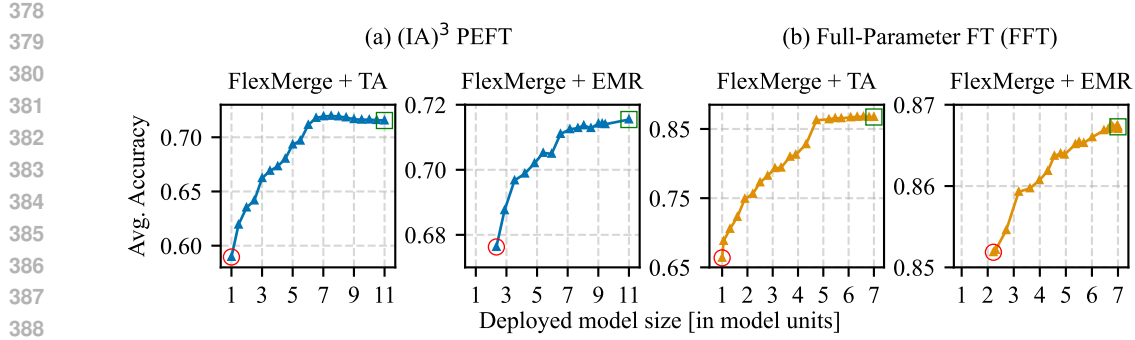


Figure 4: FLEXMERGE + TA gains 7.2% for  $(IA)^3$  going from 1 $\times$  to 3 $\times$  and more than 9% for FFT when just doubling the size from 1 $\times$  to 2 $\times$ . EMR begins with higher accuracy, yet, substantially benefits from increased size.

fine-tuning on 7 datasets sourced from (Yadav et al., 2023) (detailed in Appendix B.4). Figure 4(b) illustrates the trade-off between model size and accuracy for the T5-Large model. Here, one unit of model size corresponds to the full size of a single model. FLEXMERGE + TA gains more than 9% to reach an accuracy of 75% when just doubling the size from 1 $\times$  to 2 $\times$ . Similarly, FLEXMERGE + EMR-MERGING surpasses 86% at size 4 $\times$ , starting from 85.2% at its lowest size of 2.2 $\times$ . Consistent with our observations on vision tasks, FLEXMERGE + TA reaches very close to the fine-tuning accuracy around size 5 $\times$ , much in advance of full size 7 $\times$ . Thus, scaling the model size benefits both ends of the spectrum. Results for other combinations are included in Appendix C.3.

**Cross-algorithm analysis.** Thus far, we evaluated the accuracy-size trade-off per algorithm. We now compare algorithms at same size, yielding two interesting findings: (i) the performance gap between different algorithms significantly narrows at slightly larger sizes; and (ii) the algorithms rankings also alter in many cases, with simpler algorithms rivaling or surpassing advanced ones. This behavior aligns with the phenomenon we observed earlier: as scale increases, parameter interference between tasks reduces substantially, leading to greater natural parameter disentanglement and higher accuracy. Consequently, the explicit interference-reduction mechanisms built into advanced approaches such as TRIM in TIES or competition balancing in PCB offer marginal added benefit, because much of the interference is already mitigated simply by the increase in scale. Thus simple algorithms begin rivaling their more sophisticated counterparts at larger sizes. In Figure 5 on vision tasks, vanilla averaging exceeds TIES-MERGING at size 3.25 $\times$  while TA overlaps with PCB. While EMR-MERGING and CONSENSUS stay atop on vision, they are surpassed by PCB on PEFT at size 4.5 $\times$ . Crucially, all algorithms remain within 3 – 4% on both benchmarks at increased sizes despite originating with a

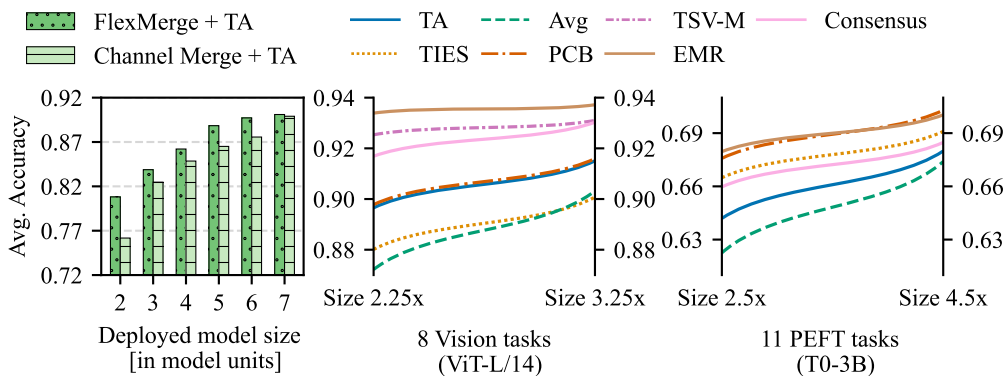


Figure 5: (Left) FLEXMERGE + TA outperforms CHANNEL MERGING + TA across all sizes. (Center, Right) Algorithm rankings shift even at modestly larger sizes, with simpler methods rivaling advanced ones. We show sizes just over CONSENSUS and EMR-MERGING’s lowest size for a wholistic comparison.

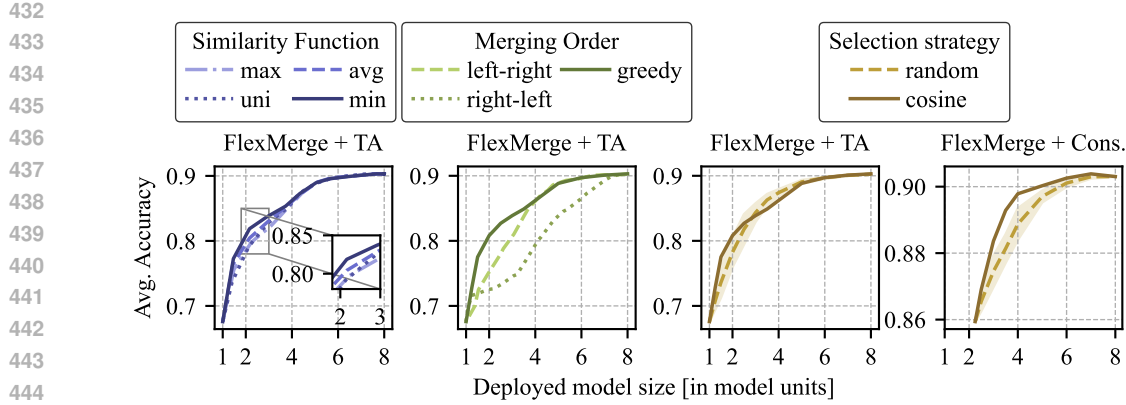


Figure 6: Ablation results for FLEXMERGE reveal that the min similarity strategy and greedy merging perform the best, while cosine similarity generally outperforms random selection.

much larger gap at size  $1\times$  (see Figure 1(b)). *Our findings provide encouraging evidence to develop and compare algorithms at sizes  $> 1\times$  rather than only at  $1\times$ .*

## 4.2 FLEXMERGE VS CHANNEL MERGING

CHANNEL MERGING (Zhang et al., 2025) uses K-Means clustering per layer, following a fixed same value of  $K$  for every layer. Each choice of  $K \in \{2, 3, \dots, M - 1\}$  results in a merged model of the corresponding size. Figure 5 charts the average accuracy with TA and ViT-B/32 for a set of integer model sizes, excluding the extremes  $1\times$  and  $8\times$  where both approaches have the identical accuracy. Recall that CHANNEL MERGING does not support fractional sizes. FLEXMERGE achieves higher accuracy than CHANNEL MERGING in all cases, thanks to its greedy pairwise merging approach which allows flexible number of groups per layer instead of restrictive clustering. Results with TIES-MERGING and visualization of clusters is included in Appendix C.5.

## 4.3 ANALYSIS

**Ablations on the merging procedure.** We ablate on the similarity functions (min, max, average, comparing unified vectors) for Equation (1) and merging orders (left-to-right, right-to-left, greedy) in FLEXMERGE using the ViT-B/32 model on 8 tasks. We also investigate random block selection over cosine similarity. Figure 6 shows that the min strategy performs the best, though other strategies are also competitive. For merging order, right to left performs the worst as expected since the final layers in neural networks tend to be more specialized and merging them first hurts accuracy. While left to right seems ideal, it can be too strict and therefore greedy emerges as the best. We further analyze the merging order of greedy in Appendix C.10. Random selection is competitive, but generally underperforms when compared across algorithm. Based on these findings, we set FLEXMERGE to use greedy with cosine similarity (min strategy) by default. For more ablations, see Appendix C.8.

**Merging and inference efficiency.** Table 2 shows that FLEXMERGE achieves highly efficient data-free merging, generating all deployed sizes in about 20 sec for up to 30 tasks. For inference with FLEXMERGE, each request follows a unique forward path through the merged model using task-specific blocks (Figure 1(a)). For a model of size  $1\times$ , all tasks share a single path, but the classification heads are always applied separately. We load the tensors of merged model (size  $> 1\times$ ) into the GPU memory once and create  $M$  task-specific model views that reference these shared tensors to process task batches in parallel. Standard merging, by contrast, processes all tasks in a single batch before splitting for task-specific heads. We simulate the worst case arrival, where inference batches corresponding to all tasks arrive at once. We consider 50 consecutive batches of size 256 (totaling 12800 samples). Each batch contains 32 samples per task across 8 tasks. Table 3 shows that FLEXMERGE maintains inference speed comparable to standard merging for both ViT-B/32 and ViT-L/14, demonstrating that larger models can enhance accuracy without slowing inference.

486  
487  
488  
Table 2: Merging time (ViT-B/32 vs  
ViT-L/14).

Method	ViT-B/32 (s)	ViT-L/14 (s)
8 Tasks		
TA (size 1x)	$\approx 0.8$	$\approx 2.6$
FLEXMERGE (all sizes)	$\approx 2.3$	$\approx 3.4$
30 Tasks		
TA (size 1x)	$\approx 1.9$	$\approx 6.1$
FLEXMERGE (all sizes)	$\approx 20$	$\approx 31$

489  
490  
491  
492  
493  
494  
495  
Table 3: Comparing inference time of FLEXMERGE against  
standard model merging. The overheads are negligible.

Model	Algorithm	Size	Inference Cost (/12800 items)
ViT-B-32	Standard Merging	1x	$12.30 \pm 0.21$ ms
	FLEXMERGE	$> 1x$	$12.21 \pm 0.41$ ms
ViT-L-14	Standard Merging	1x	$118.70 \pm 1.78$ ms
	FLEXMERGE	$> 1x$	$120.53 \pm 0.32$ ms

496  
497  
5 DISCUSSION AND CONCLUSION  
498499  
500  
501  
502  
503  
504  
505  
506  
507  
508  
509  
510  
**Benefits.** Different merging algorithms have different advantages: EMR and CONSENSUS achieve high accuracy but require task-specific reconstruction during inference, incurring overheads. FLEXMERGE can also mitigate this overhead as larger deployed models need fewer blocks to be reconstructed (see Appendix C.9). In contrast, TIES and TA avoid reconstruction but have lower accuracy. FLEXMERGE provides flexibility, letting practitioners choose algorithms and balance accuracy, reconstruction overhead, and model size for various deployment scenarios.511  
512  
513  
514  
515  
**Limitations.** Most works, including FLEXMERGE, are limited to merging models with the same architecture as merging heterogeneous models remains challenging (Singh & Jaggi, 2020; Imfeld et al., 2024). Secondly, the theoretical insights for effective model merging are limited (Ortiz-Jimenez et al., 2023). For FLEXMERGE, how to obtain the optimal merged model for any given size remains unclear. Although extensive ablations help guide (Section 4.3), further investigation is needed to understand the bounds of the accuracy-size trade-off.516  
517  
518  
519  
520  
521  
522  
523  
524  
525  
526  
527  
528  
529  
530  
531  
532  
533  
534  
535  
536  
537  
538  
539  
We introduced FLEXMERGE, a flexible, data-free model merging framework that extends beyond traditional single-model fusion and offers precise control over fused model size. Extensive experiments show that the accuracy-size trade-off exhibits favorable properties for several algorithms, benefiting from rapid accuracy gains with modest size increments. Future work may explore specialized algorithms for block-level merging.540  
541  
REFERENCES

M Israk Ahmed, Shahriyar Mahmud Mamun, and Asif Uz Zaman Asif. Dcnn-based vegetable image classification using transfer learning: A comparative study. In *2021 5th International Conference on Computer, Communication and Signal Processing (ICCCSP)*, pp. 235–243. IEEE, 2021.

Sarder Iftekhar Ahmed, Muhammad Ibrahim, Md Nadim, Md Mizanur Rahman, Maria Mehjabin Shejunti, Taskeed Jabid, and Md Sawkat Ali. Mangoleafbd: A comprehensive image dataset to classify diseased and healthy mango leaves. *Data in Brief*, 47:108941, 2023.

Stephen H Bach, Victor Sanh, Zheng-Xin Yong, Albert Webson, Colin Raffel, Nihal V Nayak, Abheesht Sharma, Taewoon Kim, M Saiful Bari, Thibault Fevry, et al. Promptsource: An integrated development environment and repository for natural language prompts. *arXiv preprint arXiv:2202.01279*, 2022.

Satanjeev Banerjee and Alon Lavie. METEOR: An automatic metric for MT evaluation with improved correlation with human judgments. In Jade Goldstein, Alon Lavie, Chin-Yew Lin, and Clare Voss (eds.), *Proceedings of the ACL Workshop on Intrinsic and Extrinsic Evaluation Measures for Machine Translation and/or Summarization*, pp. 65–72, Ann Arbor, Michigan, June 2005. Association for Computational Linguistics. URL <https://aclanthology.org/W05-0909/>.

Puneet Bansal. Intel image classification. Available on <https://www.kaggle.com/puneet6060/intel-image-classification>, Online, 2019.

Rishi Bommasani, Drew A Hudson, Ehsan Adeli, Russ Altman, Simran Arora, Sydney von Arx, Michael S Bernstein, Jeannette Bohg, Antoine Bosselut, Emma Brunskill, et al. On the opportunities and risks of foundation models. *arXiv preprint arXiv:2108.07258*, 2021.

540 Lukas Bossard, Matthieu Guillaumin, and Luc Van Gool. Food-101 – Mining Discriminative  
 541 Components with Random Forests. In *IEEE European Conference on Computer Vision (ECCV)*,  
 542 2014.

543

544 CCHANG. Garbage classification. <https://www.kaggle.com/ds/81794>, 2018.

545 Junbum Cha, Sanghyuk Chun, Kyungjae Lee, Han-Cheol Cho, Seunghyun Park, Yunsung Lee,  
 546 and Sungrae Park. SWAD: domain generalization by seeking flat minima. In Marc’Aurelio  
 547 Ranzato, Alina Beygelzimer, Yann N. Dauphin, Percy Liang, and Jennifer Wortman Vaughan  
 548 (eds.), *Advances in Neural Information Processing Systems 34: Annual Conference on Neural  
 549 Information Processing Systems 2021, NeurIPS 2021, December 6-14, 2021, virtual*, pp. 22405–  
 550 22418, 2021. URL <https://proceedings.neurips.cc/paper/2021/hash/bcb41ccdc4363c6848a1d760f26c28a0-Abstract.html>.

551

552 Gong Cheng, Junwei Han, and Xiaoqiang Lu. Remote sensing image scene classification: Benchmark  
 553 and state of the art. *Proceedings of the IEEE*, 105(10):1865–1883, 2017.

554

555 Mircea Cimpoi, Subhransu Maji, Iasonas Kokkinos, Sammy Mohamed, and Andrea Vedaldi. Describing  
 556 textures in the wild. In *Proceedings of the IEEE conference on computer vision and pattern  
 557 recognition*, pp. 3606–3613, 2014.

558

559 Tarin Clanuwat, Mikel Bober-Irizar, Asanobu Kitamoto, Alex Lamb, Kazuaki Yamamoto, and David  
 560 Ha. Deep learning for classical Japanese literature. *arXiv*, 2018. URL <http://arxiv.org/abs/1812.01718v1>.

561

562 Adam Coates, Andrew Ng, and Honglak Lee. An analysis of single-layer networks in unsupervised  
 563 feature learning. In *International Conference on Artificial Intelligence and Statistics (AISTATS)*,  
 564 2011. <https://proceedings.mlr.press/v15/coates11a.html>.

565

566 Gregory Cohen, Saeed Afshar, Jonathan Tapson, and Andre Van Schaik. EMNIST: Extending MNIST  
 567 to handwritten letters. In *International Joint Conference on Neural Networks (IJCNN)*, 2017.

568

569 Thomas H. Cormen, Charles E. Leiserson, Ronald L. Rivest, and Clifford Stein. *Introduction to  
 570 Algorithms, Third Edition*. The MIT Press, 3rd edition, 2009. ISBN 0262033844.

571

572 Marie-Catherine De Marneffe, Mandy Simons, and Judith Tonhauser. The commitmentbank: In-  
 573 vestigating projection in naturally occurring discourse. In *proceedings of Sinn und Bedeutung*,  
 574 volume 23, pp. 107–124, 2019.

575

576 DeepNets. Landscape recognition. <https://www.kaggle.com/datasets/utkarshsaxenadn/landscape-recognition-image-dataset-12k-images>.

577

578 Jia Deng, Wei Dong, Richard Socher, Li-Jia Li, Kai Li, and Li Fei-Fei. Imagenet: A large-scale hier-  
 579 archical image database. In *2009 IEEE Conference on Computer Vision and Pattern Recognition*,  
 580 pp. 248–255, 2009. doi: 10.1109/CVPR.2009.5206848.

581

582 Jacob Devlin, Ming-Wei Chang, Kenton Lee, and Kristina Toutanova. Bert: Pre-training of deep  
 583 bidirectional transformers for language understanding. *arXiv preprint arXiv:1810.04805*, 2018.

584

585 Jesse Dodge, Gabriel Ilharco, Roy Schwartz, Ali Farhadi, Hannaneh Hajishirzi, and Noah Smith.  
 586 Fine-tuning pretrained language models: Weight initializations, data orders, and early stopping.  
 587 *arXiv preprint arXiv:2002.06305*, 2020.

588

589 Alexey Dosovitskiy, Lucas Beyer, Alexander Kolesnikov, Dirk Weissenborn, Xiaohua Zhai, Thomas  
 590 Unterthiner, Mostafa Dehghani, Matthias Minderer, Georg Heigold, Sylvain Gelly, Jakob Uszkoreit,  
 591 and Neil Houlsby. An image is worth 16x16 words: Transformers for image recognition at scale.  
 592 In *Proceedings of the International Conference on Learning Representations (ICLR)*, 2021.

593

594 Guodong Du, Junlin Lee, Jing Li, Runhua Jiang, Yifei Guo, Shuyang Yu, Hanting Liu, Sim Kuan  
 595 Goh, Ho-Kin Tang, Daojing He, and Min Zhang. Parameter competition balancing for model  
 596 merging. In *The Thirty-eighth Annual Conference on Neural Information Processing Systems*,  
 597 2024. URL <https://openreview.net/forum?id=15SbRtvSRS>.

594 Chris Fifty, Ehsan Amid, Zhe Zhao, Tianhe Yu, Rohan Anil, and Chelsea Finn. Efficiently identifying  
 595 task groupings for multi-task learning. *Advances in Neural Information Processing Systems*, 34:  
 596 27503–27516, 2021.

597 Antonio Andrea Gargiulo, Donato Crisostomi, Maria Sofia Bucarelli, Simone Scardapane, Fabrizio  
 598 Silvestri, and Emanuele Rodola. Task singular vectors: Reducing task interference in model  
 599 merging. In *Proceedings of the Computer Vision and Pattern Recognition Conference*, pp. 18695–  
 600 18705, 2025.

601 Danilo Giampiccolo, Bernardo Magnini, Ido Dagan, and William B Dolan. The third pascal rec-  
 602 ognizing textual entailment challenge. In *Proceedings of the ACL-PASCAL workshop on textual*  
 603 *entailment and paraphrasing*, pp. 1–9, 2007.

604 Ian J Goodfellow, Dumitru Erhan, Pierre Luc Carrier, Aaron Courville, Mehdi Mirza, Ben Hamner,  
 605 Will Cukierski, Yichuan Tang, David Thaler, Dong-Hyun Lee, et al. Challenges in representation  
 606 learning: A report on three machine learning contests. In *International Conference on Neural*  
 607 *Information Processing (ICONIP)*, 2013. URL <http://arxiv.org/abs/1307.0414v1>.

608 Vipul Gupta, Santiago Akle Serrano, and Dennis DeCoste. Stochastic weight averaging in parallel:  
 609 Large-batch training that generalizes well. In *8th International Conference on Learning Repre-  
 610 sentations, ICLR 2020, Addis Ababa, Ethiopia, April 26-30, 2020*. OpenReview.net, 2020. URL  
 611 <https://openreview.net/forum?id=rygFWAEFwS>.

612 Patrick Helber, Benjamin Bischke, Andreas Dengel, and Damian Borth. Eurosat: A novel dataset  
 613 and deep learning benchmark for land use and land cover classification. *IEEE Journal of Selected*  
 614 *Topics in Applied Earth Observations and Remote Sensing*, 12(7):2217–2226, 2019.

615 Chenyu Huang, Peng Ye, Tao Chen, Tong He, Xiangyu Yue, and Wanli Ouyang. EMR-merging:  
 616 Tuning-free high-performance model merging. In *The Thirty-eighth Annual Conference on Neural*  
 617 *Information Processing Systems*, 2024. URL <https://openreview.net/forum?id=1Ydjzx3DYu>.

618 Gabriel Ilharco, Marco Túlio Ribeiro, Mitchell Wortsman, Ludwig Schmidt, Hannaneh Hajishirzi,  
 619 and Ali Farhadi. Editing models with task arithmetic. In *The Eleventh International Conference on*  
 620 *Learning Representations*, 2023. URL <https://openreview.net/forum?id=6t0Kwf8-jrj>.

621 Moritz Imfeld, Jacopo Graldi, Marco Giordano, Thomas Hofmann, Sotiris Anagnostidis, and  
 622 Sidak Pal Singh. Transformer fusion with optimal transport. In *The Twelfth International Confer-  
 623 ence on Learning Representations*, 2024. URL <https://openreview.net/forum?id=LjeqMvOpen>.

624 Pavel Izmailov, Dmitrii Podoprikhin, Timur Garipov, Dmitry P. Vetrov, and Andrew Gordon Wilson.  
 625 Averaging weights leads to wider optima and better generalization. In Amir Globerson and Ricardo  
 626 Silva (eds.), *Proceedings of the Thirty-Fourth Conference on Uncertainty in Artificial Intelligence,  
 627 UAI 2018, Monterey, California, USA, August 6-10, 2018*, pp. 876–885. AUAI Press, 2018. URL  
 628 <http://auai.org/uai2018/proceedings/papers/313.pdf>.

629 Mona Jalal, Kaihong Wang, Sankara Jefferson, Yi Zheng, Elaine O Nsoesie, and Margrit Betke.  
 630 Scraping social media photos posted in kenya and elsewhere to detect and analyze food types. In  
 631 *Proceedings of the 5th International Workshop on Multimedia Assisted Dietary Management*, pp.  
 632 50–59, 2019.

633 Ruochen Jin, Bojian Hou, Jiancong Xiao, Weijie J Su, and Li Shen. Fine-tuning attention modules  
 634 only: Enhancing weight disentanglement in task arithmetic. In *The Thirteenth International*  
 635 *Conference on Learning Representations*, 2025.

636 Xisen Jin, Xiang Ren, Daniel Preotiuc-Pietro, and Pengxiang Cheng. Dataless knowledge fusion  
 637 by merging weights of language models. In *The Eleventh International Conference on Learning*  
 638 *Representations*, 2023. URL <https://openreview.net/forum?id=FCn0huR6AnM>.

639 Aditya Khosla, Nityananda Jayadevaprakash, Bangpeng Yao, and Li Fei-Fei. Novel dataset for  
 640 fine-grained image categorization. In *First Workshop on Fine-Grained Visual Categorization, IEEE*  
 641 *Conference on Computer Vision and Pattern Recognition*, Colorado Springs, CO, June 2011.

648 Tushar Khot, Peter Clark, Michal Guerquin, Peter Jansen, and Ashish Sabharwal. Qasc: A dataset for  
 649 question answering via sentence composition. *Proceedings of the AAAI Conference on Artificial*  
 650 *Intelligence*, 34(05):8082–8090, Apr. 2020. doi: 10.1609/aaai.v34i05.6319. URL <https://ojs.aaai.org/index.php/AAAI/article/view/6319>.

652  
 653 Donald Ervin Knuth. *The art of computer programming*, volume 3. Pearson Education, 1997.

654 Jakub Konečný, H. Brendan McMahan, Daniel Ramage, and Peter Richtárik. Federated optimization:  
 655 Distributed machine learning for on-device intelligence. *CoRR*, abs/1610.02527, 2016. URL  
 656 <http://arxiv.org/abs/1610.02527>.

657  
 658 Jonathan Krause, Michael Stark, Jia Deng, and Li Fei-Fei. 3d object representations for fine-grained  
 659 categorization. In *Proceedings of the IEEE international conference on computer vision workshops*,  
 660 pp. 554–561, 2013.

661 Alex Krizhevsky, Geoffrey Hinton, et al. Learning multiple layers of features from tiny images, 2009.  
 662 <https://www.cs.toronto.edu/~kriz/learning-features-2009-TR.pdf>.

663  
 664 Makerere AI Lab. Bean disease dataset, January 2020. URL <https://github.com/AI-Lab-Makerere/ibean/>.

665  
 666 Yann LeCun. The mnist database of handwritten digits. <http://yann.lecun.com/exdb/mnist/>, 1998.

667  
 668 Yeoreum Lee, Jinwook Jung, and Sungyong Baik. Mitigating parameter interference in model  
 669 merging via sharpness-aware fine-tuning. In *The Thirteenth International Conference on Learning*  
 670 *Representations*, 2025. URL <https://openreview.net/forum?id=eaTqsptDPL>.

671  
 672 Hector Levesque, Ernest Davis, and Leora Morgenstern. The winograd schema challenge. In  
 673 *Thirteenth international conference on the principles of knowledge representation and reasoning*,  
 674 2012.

675 Chin-Yew Lin. ROUGE: A package for automatic evaluation of summaries. In *Text Summarization*  
 676 *Branches Out*, pp. 74–81, Barcelona, Spain, July 2004. Association for Computational Linguistics.  
 677 URL <https://aclanthology.org/W04-1013/>.

678  
 679 Tsung-Yi Lin, Michael Maire, Serge Belongie, James Hays, Pietro Perona, Deva Ramanan, Piotr  
 680 Dollár, and C. Lawrence Zitnick. Microsoft coco: Common objects in context. In David Fleet,  
 681 Tomas Pajdla, Bernt Schiele, and Tinne Tuytelaars (eds.), *Computer Vision – ECCV 2014*, pp.  
 682 740–755, Cham, 2014. Springer International Publishing. ISBN 978-3-319-10602-1.

683  
 684 Haokun Liu, Derek Tam, Mohammed Muqeeth, Jay Mohta, Tenghao Huang, Mohit Bansal, and  
 685 Colin A Raffel. Few-shot parameter-efficient fine-tuning is better and cheaper than in-context  
 686 learning. *Advances in Neural Information Processing Systems (NeurIPS)*, 35:1950–1965, 2022.

687  
 688 Zhenyi Lu, Chenghao Fan, Wei Wei, Xiaoye Qu, Dangyang Chen, and Yu Cheng. Twin-merging:  
 689 Dynamic integration of modular expertise in model merging. In *The Thirty-eighth Annual Conference*  
 690 *on Neural Information Processing Systems*, 2024. URL <https://openreview.net/forum?id=81YIt63TTn>.

691  
 692 TorchVision maintainers and contributors. Torchvision: Pytorch’s computer vision library. <https://github.com/pytorch/vision>, 2016.

693  
 694 Michael S Matena and Colin Raffel. Merging models with fisher-weighted averaging. In Alice H. Oh,  
 695 Alekh Agarwal, Danielle Belgrave, and Kyunghyun Cho (eds.), *Advances in Neural Information*  
 696 *Processing Systems*, 2022. URL [https://openreview.net/forum?id=LSK1p\\_ace0C](https://openreview.net/forum?id=LSK1p_ace0C).

697  
 698 Brendan McMahan, Eider Moore, Daniel Ramage, Seth Hampson, and Blaise Agüera y Arcas.  
 699 Communication-efficient learning of deep networks from decentralized data. In Aarti Singh  
 700 and Xiaojin (Jerry) Zhu (eds.), *Proceedings of the 20th International Conference on Artificial*  
 701 *Intelligence and Statistics, AISTATS 2017, 20-22 April 2017, Fort Lauderdale, FL, USA*, volume 54  
 of *Proceedings of Machine Learning Research*, pp. 1273–1282. PMLR, 2017. URL <http://proceedings.mlr.press/v54/mcmahan17a.html>.

702 Yixin Nie, Adina Williams, Emily Dinan, Mohit Bansal, Jason Weston, and Douwe Kiela. Adversarial  
 703 nli: A new benchmark for natural language understanding. *arXiv preprint arXiv:1910.14599*, 2019.  
 704

705 Maria-Elena Nilsback and Andrew Zisserman. Automated flower classification over a large number  
 706 of classes. In *2008 Sixth Indian conference on computer vision, graphics & image processing*,  
 707 2008.

708 Guillermo Ortiz-Jimenez, Alessandro Favero, and Pascal Frossard. Task arithmetic in the tangent  
 709 space: Improved editing of pre-trained models. In *Thirty-seventh Conference on Neural Information  
 710 Processing Systems*, 2023. URL <https://openreview.net/forum?id=0A9f2jZDGW>.  
 711

712 Kishore Papineni, Salim Roukos, Todd Ward, and Wei-Jing Zhu. Bleu: a method for automatic  
 713 evaluation of machine translation. In *Proceedings of the 40th Annual Meeting on Association for  
 714 Computational Linguistics, ACL '02*, pp. 311–318, USA, 2002. Association for Computational  
 715 Linguistics. doi: 10.3115/1073083.1073135. URL <https://doi.org/10.3115/1073083.1073135>.  
 716

717 Omkar M Parkhi, Andrea Vedaldi, Andrew Zisserman, and CV Jawahar. Cats and dogs. In *IEEE  
 718 Conference on Computer Vision and Pattern Recognition (CVPR)*, 2012.  
 719

720 Mohammad Taher Pilehvar and Jose Camacho-Collados. Wic: the word-in-context dataset for  
 721 evaluating context-sensitive meaning representations. *arXiv preprint arXiv:1808.09121*, 2018.  
 722

723 Konstantin Pogorelov, Kristin Ranheim Randel, Carsten Griwodz, Sigrun Losada Eskeland, Thomas  
 724 de Lange, Dag Johansen, Concetto Spampinato, Duc-Tien Dang-Nguyen, Mathias Lux, Peter The-  
 725 lin Schmidt, et al. Kvasir: A multi-class image dataset for computer aided gastrointestinal disease  
 726 detection. In *Proceedings of the 8th ACM on Multimedia Systems Conference*, pp. 164–169, 2017.  
 727

728 Alec Radford, Jeffrey Wu, Rewon Child, David Luan, Dario Amodei, and Ilya Sutskever. Language  
 729 Models are Unsupervised Multitask Learners, 2019. <https://openai.com/blog/better-language-models/>.  
 730

731 Alec Radford, Jong Wook Kim, Chris Hallacy, Aditya Ramesh, Gabriel Goh, Sandhini Agarwal,  
 732 Girish Sastry, Amanda Askell, Pamela Mishkin, Jack Clark, et al. Learning transferable visual  
 733 models from natural language supervision. In *International conference on machine learning*, pp.  
 734 8748–8763. PMLR, 2021.

735 Colin Raffel, Noam Shazeer, Adam Roberts, Katherine Lee, Sharan Narang, Michael Matena, Yanqi  
 736 Zhou, Wei Li, and Peter J Liu. Exploring the limits of transfer learning with a unified text-to-text  
 737 transformer. *Journal of Machine Learning Research (JMLR)*, 21(140):1–67, 2020.  
 738

739 Melissa Roemmele, Cosmin Adrian Bejan, and Andrew S Gordon. Choice of plausible alternatives:  
 740 An evaluation of commonsense causal reasoning. In *2011 AAAI Spring Symposium Series*, 2011.  
 741

742 Keisuke Sakaguchi, Ronan Le Bras, Chandra Bhagavatula, and Yejin Choi. Winogrande: An  
 743 adversarial winograd schema challenge at scale. *Communications of the ACM*, 64(9):99–106,  
 744 2021.

745 Victor Sanh, Albert Webson, Colin Raffel, Stephen Bach, Lintang Sutawika, Zaid Alyafeai, Antoine  
 746 Chaffin, Arnaud Stiegler, Arun Raja, Manan Dey, M Saiful Bari, Canwen Xu, Urmish Thakker,  
 747 Shanya Sharma Sharma, Eliza Szczechla, Taewoon Kim, Gunjan Chhablani, Nihal Nayak, De-  
 748 bajyoti Datta, Jonathan Chang, Mike Tian-Jian Jiang, Han Wang, Matteo Manica, Sheng Shen,  
 749 Zheng Xin Yong, Harshit Pandey, Rachel Bawden, Thomas Wang, Trishala Neeraj, Jos Rozen,  
 750 Abheesh Sharma, Andrea Santilli, Thibault Fevry, Jason Alan Fries, Ryan Teehan, Teven Le Scao,  
 751 Stella Biderman, Leo Gao, Thomas Wolf, and Alexander M Rush. Multitask prompted training  
 752 enables zero-shot task generalization. In *International Conference on Learning Representations*,  
 753 2022. URL <https://openreview.net/forum?id=9Vrb9D0WI4>.  
 754

755 Rishi Sharma, James Allen, Omid Bakhshandeh, and Nasrin Mostafazadeh. Tackling the story ending  
 756 biases in the story cloze test. In *Proceedings of the 56th Annual Meeting of the Association for  
 757 Computational Linguistics (Volume 2: Short Papers)*, pp. 752–757, 2018.

756 R. Sibson. Slink: An optimally efficient algorithm for the single-link cluster method. *The Computer*  
 757 *Journal*, 16(1):30–34, 01 1973. ISSN 0010-4620. doi: 10.1093/comjnl/16.1.30. URL <https://doi.org/10.1093/comjnl/16.1.30>.

759  
 760 Sidak Pal Singh and Martin Jaggi. Model fusion via optimal transport. In H. Larochelle, M. Ranzato,  
 761 R. Hadsell, M.F. Balcan, and H. Lin (eds.), *Advances in Neural Information Processing Systems*,  
 762 volume 33, pp. 22045–22055. Curran Associates, Inc., 2020. URL [https://proceedings.neurips.cc/paper\\_files/paper/2020/file/fb2697869f56484404c8ceee2985b01d-Paper.pdf](https://proceedings.neurips.cc/paper_files/paper/2020/file/fb2697869f56484404c8ceee2985b01d-Paper.pdf).

764  
 765 Richard Socher, Alex Perelygin, Jean Wu, Jason Chuang, Christopher D Manning, Andrew Ng,  
 766 and Christopher Potts. Recursive deep models for semantic compositionality over a sentiment  
 767 treebank. In *Empirical Methods in Natural Language Processing (EMNLP)*, 2013. <https://aclanthology.org/D13-1170/>.

769  
 770 Johannes Stallkamp, Marc Schlipsing, Jan Salmen, and Christian Igel. The german traffic sign  
 771 recognition benchmark: a multi-class classification competition. In *The 2011 international joint*  
 772 *conference on neural networks*, pp. 1453–1460. IEEE, 2011.

775  
 776 Trevor Standley, Amir Zamir, Dawn Chen, Leonidas Guibas, Jitendra Malik, and Silvio Savarese.  
 777 Which tasks should be learned together in multi-task learning? In *International conference on*  
 778 *machine learning*, pp. 9120–9132. PMLR, 2020.

779  
 780 George Stoica, Pratik Ramesh, Boglarka Ecsedi, Leshem Choshen, and Judy Hoffman. Model  
 781 merging with svd to tie the knots. In *The Thirteenth International Conference on Learning*  
 782 *Representations*, 2025.

783  
 784 Alane Suhr, Stephanie Zhou, Ally Zhang, Iris Zhang, Huajun Bai, and Yoav Artzi. A corpus for  
 785 reasoning about natural language grounded in photographs, 2019. URL <https://arxiv.org/abs/1811.00491>.

786  
 787 Oyvind Tafjord, Matt Gardner, Kevin Lin, and Peter Clark. QuaRTz: An open-domain dataset of  
 788 qualitative relationship questions. In Kentaro Inui, Jing Jiang, Vincent Ng, and Xiaojun Wan (eds.),  
 789 *Proceedings of the 2019 Conference on Empirical Methods in Natural Language Processing and*  
 790 *the 9th International Joint Conference on Natural Language Processing (EMNLP-IJCNLP)*, pp.  
 791 5941–5946, Hong Kong, China, November 2019. Association for Computational Linguistics. doi:  
 792 10.18653/v1/D19-1608. URL <https://aclanthology.org/D19-1608/>.

793  
 794 Anke Tang, Li Shen, Yong Luo, Nan Yin, Lefei Zhang, and Dacheng Tao. Merging multi-task models  
 795 via weight-ensembling mixture of experts. In *Forty-first International Conference on Machine*  
 796 *Learning*, 2024a. URL <https://openreview.net/forum?id=nLRKn074RB>.

797  
 798 Anke Tang, Li Shen, Yong Luo, Yibing Zhan, Han Hu, Bo Du, Yixin Chen, and Dacheng Tao.  
 799 Parameter-efficient multi-task model fusion with partial linearization. In *The Twelfth International*  
 800 *Conference on Learning Representations*, 2024b.

801  
 802 Simon Vandenhende, Stamatios Georgoulis, Wouter Van Gansbeke, Marc Proesmans, Dengxin Dai,  
 803 and Luc Van Gool. Multi-task learning for dense prediction tasks: A survey. *IEEE transactions on*  
 804 *pattern analysis and machine intelligence*, 44(7):3614–3633, 2021.

805  
 806 Ramakrishna Vedantam, C. Lawrence Zitnick, and Devi Parikh. Cider: Consensus-based image  
 807 description evaluation. In *2015 IEEE Conference on Computer Vision and Pattern Recognition*  
 808 (*CVPR*), pp. 4566–4575, 2015. doi: 10.1109/CVPR.2015.7299087.

809  
 810 Bastiaan S Veeling, Jasper Linmans, Jim Winkens, Taco Cohen, and Max Welling. Rotation equivariant  
 811 CNNs for digital pathology. In *International Conference on Medical Image Computing and*  
 812 *Computer Assisted Intervention (MICCAI)*, 2018. URL <https://arxiv.org/abs/1806.03962>  
 813 v1.

814  
 815 Ke Wang, Nikolaos Dimitriadis, Guillermo Ortiz-Jimenez, François Fleuret, and Pascal Frossard.  
 816 Localizing task information for improved model merging and compression. In *Forty-first Interna-*  
 817 *tional Conference on Machine Learning*, 2024. URL <https://openreview.net/forum?id=DWT9uiGjxt>.

810 Ke Wang, Nikolaos Dimitriadis, Alessandro Favero, Guillermo Ortiz-Jimenez, François Fleuret,  
 811 and Pascal Frossard. Lines: Post-training layer scaling prevents forgetting and enhances model  
 812 merging. In *The Thirteenth International Conference on Learning Representations*, 2025.

813

814 Wenhui Wang, Hangbo Bao, Li Dong, Johan Bjorck, Zhiliang Peng, Qiang Liu, Kriti Aggarwal,  
 815 Owais Khan Mohammed, Saksham Singhal, Subhajit Som, and Furu Wei. Image as a foreign  
 816 language: Beit pretraining for all vision and vision-language tasks, 2022. URL <https://arxiv.org/abs/2208.10442>.

817

818 Thomas Wolf, Lysandre Debut, Victor Sanh, Julien Chaumond, Clement Delangue, Anthony Moi,  
 819 Pierrick Cistac, Tim Rault, Rémi Louf, Morgan Funtowicz, et al. Huggingface’s transformers:  
 820 State-of-the-art natural language processing. *arXiv preprint arXiv:1910.03771*, 2019.

821

822 Mitchell Wortsman, Gabriel Ilharco, Samir Ya Gadre, Rebecca Roelofs, Raphael Gontijo-Lopes,  
 823 Ari S Morcos, Hongseok Namkoong, Ali Farhadi, Yair Carmon, Simon Kornblith, et al. Model  
 824 soups: averaging weights of multiple fine-tuned models improves accuracy without increasing  
 825 inference time. In *Proceedings of the International Conference on Machine Learning (ICML)*, pp.  
 826 23965–23998, 2022.

827

828 Haixia Xiao, Feng Zhang, Zhongping Shen, Kun Wu, and Jinglin Zhang. Classification of weather  
 829 phenomenon from images by using deep convolutional neural network. *Earth and Space Science*,  
 830 8(5):e2020EA001604, 2021.

831

832 Han Xiao, Kashif Rasul, and Roland Vollgraf. Fashion-mnist: a novel image dataset for benchmarking  
 833 machine learning algorithms. *arXiv*, 2017. URL <http://arxiv.org/abs/1708.07747v2>.

834

835 Jianxiong Xiao, James Hays, Krista A Ehinger, Aude Oliva, and Antonio Torralba. Sun database:  
 836 Large-scale scene recognition from abbey to zoo. In *2010 IEEE computer society conference on  
 837 computer vision and pattern recognition*, pp. 3485–3492. IEEE, 2010.

838

839 Prateek Yadav, Derek Tam, Leshem Choshen, Colin A Raffel, and Mohit Bansal. Ties-merging:  
 840 Resolving interference when merging models. In A. Oh, T. Naumann, A. Globerson, K. Saenko,  
 841 M. Hardt, and S. Levine (eds.), *Advances in Neural Information Processing Systems*, volume 36,  
 842 pp. 7093–7115. Curran Associates, Inc., 2023. URL [https://proceedings.neurips.cc/paper\\_files/paper/2023/file/1644c9af28ab7916874f6fd6228a9bcf-Paper-Conference.pdf](https://proceedings.neurips.cc/paper_files/paper/2023/file/1644c9af28ab7916874f6fd6228a9bcf-Paper-Conference.pdf).

843

844 Enneng Yang, Li Shen, Zhenyi Wang, Guibing Guo, Xiaojun Chen, Xingwei Wang, and Dacheng  
 845 Tao. Representation surgery for multi-task model merging. In Ruslan Salakhutdinov, Zico  
 846 Kolter, Katherine Heller, Adrian Weller, Nuria Oliver, Jonathan Scarlett, and Felix Berkenkamp  
 847 (eds.), *Proceedings of the 41st International Conference on Machine Learning*, volume 235 of  
 848 *Proceedings of Machine Learning Research*, pp. 56332–56356. PMLR, 21–27 Jul 2024a. URL  
 849 <https://proceedings.mlr.press/v235/yang24t.html>.

850

851 Enneng Yang, Zhenyi Wang, Li Shen, Shiwei Liu, Guibing Guo, Xingwei Wang, and Dacheng  
 852 Tao. Adamerging: Adaptive model merging for multi-task learning. In *The Twelfth International  
 853 Conference on Learning Representations*, 2024b. URL <https://openreview.net/forum?id=nZP6NgD3QY>.

854

855 Yi Yang, Wen-tau Yih, and Christopher Meek. WikiQA: A challenge dataset for open-domain  
 856 question answering. In Lluís Màrquez, Chris Callison-Burch, and Jian Su (eds.), *Proceedings of the  
 857 2015 Conference on Empirical Methods in Natural Language Processing*, pp. 2013–2018, Lisbon,  
 858 Portugal, September 2015. Association for Computational Linguistics. doi: 10.18653/v1/D15-1237.  
 859 URL <https://aclanthology.org/D15-1237/>.

860

861 Le Yu, Bowen Yu, Haiyang Yu, Fei Huang, and Yongbin Li. Language models are super mario:  
 862 Absorbing abilities from homologous models as a free lunch. In *Forty-first International Conference  
 863 on Machine Learning*, 2024.

864

865 Netzer Yuval. Reading digits in natural images with unsupervised feature learning. In *Proceedings of  
 866 the NIPS Workshop on Deep Learning and Unsupervised Feature Learning*, 2011.

864 Rowan Zellers, Ari Holtzman, Yonatan Bisk, Ali Farhadi, and Yejin Choi. Hellaswag: Can a machine  
 865 really finish your sentence? *arXiv preprint arXiv:1905.07830*, 2019.

866

867 Mingyang Zhang, Jing Liu, Ganggui Ding, Linlin Ou, Xinyi Yu, and Bohan Zhuang. Channel  
 868 merging: Preserving specialization for merged experts. *Proceedings of the AAAI Conference on*  
 869 *Artificial Intelligence*, 39(21):22479–22487, Apr. 2025. doi: 10.1609/aaai.v39i21.34405. URL  
 870 <https://ojs.aaai.org/index.php/AAAI/article/view/34405>.

871

872 Yuan Zhang, Jason Baldridge, and Luheng He. PAWS: Paraphrase adversaries from word scrambling.  
 873 In Jill Burstein, Christy Doran, and Thamar Solorio (eds.), *Proceedings of the 2019 Conference of*  
 874 *the North American Chapter of the Association for Computational Linguistics: Human Language*  
 875 *Technologies, Volume 1 (Long and Short Papers)*, pp. 1298–1308, Minneapolis, Minnesota, June  
 876 2019. Association for Computational Linguistics. doi: 10.18653/v1/N19-1131. URL <https://aclanthology.org/N19-1131/>.

877

878 Ziyu Zhao, Tao Shen, Didi Zhu, Zexi Li, Jing Su, Xuwu Wang, and Fei Wu. Merging loras like  
 879 playing lego: Pushing the modularity of lora to extremes through rank-wise clustering. In *The*  
 880 *Thirteenth International Conference on Learning Representations*, 2025.

881

882

883

884

885

886

887

888

889

890

891

892

893

894

895

896

897

898

899

900

901

902

903

904

905

906

907

908

909

910

911

912

913

914

915

916

917